NATIONAL ADVISORY COMMITTEE FOR AERONAUTICS

TECHNICAL NOTE

No. 1370

CORRELATION OF EXPERIMENTAL AND CALCULATED EFFECTS OF

PRODUCT OF INERTIA ON LATERAL STABILITY

By Marion O. McKinney, Jr. and Hubert M. Drake

Langley Memorial Aeronautical Laboratory
Langley Field, Va.

Washington
July 1947

AFMDC
TECHNICAL LIBRARY
AFL 2811

THE ARMY LIBRARY
WASHINGTON, D. C.

JUL 24 1947

NATIONAL ADVISORY COMMITTEE FOR AERONAUTICS

TECHNICAL NOTE NO. 1370

CORRELATION OF EXPERIMENTAL AND CALCULATED EFFECTS OF

PRODUCT OF INERTIA ON LATERAL STABILITY

By Marion O. McKinney, Jr. and Hubert M. Drake

SUMMARY

A correlation of experimental and calculated effects of the
product of inertia on the stability of the lateral oscillations of
airplanes has been obtained from flight tests of a free-flying air-
plane model having a 42° sweptback wing and from calculations of the
stability of the model. In order to provide a comprehensive correla-
tion, the static directional stability of the model was varied by
changing the vertical-tail area and tail length and the inclination
of the longitudinal principal axis of inertia relative to the wind
axis was varied by changing the wing incidence.

The calculated lateral-stability boundaries were found to be
in good agreement with measured lateral stability when the product-
of-inertia terms were included in the calculations. Neglecting the
product of inertia, however, led to wide discrepancies between
calculated and measured stability. These results emphasized the
necessity for considering the product of inertia in lateral-stability
analyses.

The general flying characteristics were influenced primarily
by the static directional stability and to a lesser degree by the
stability of the lateral oscillations. A certain minimum amount
of static directional stability was required to give good controlla-
bility even when less directional stability provided good damping
of the lateral oscillations.

INTRODUCTION

Until recently the effects of the product of inertia usually
have been neglected in lateral-stability analyses because the
lateral-stability studies of reference 1 indicated that these
effects were relatively unimportant for conventional airplanes.
Calculations in reference 2, however, show that the product of
inertia may have a pronounced effect on the lateral stability of
some high-speed airplanes because of high wing loadings, large

differences between yawing and rolling moments of inertia, high
operational altitudes, and sweepback. The sweepback may cause
high effective dihedral and high angles of attack and, consequently,
large angles between the principal longitudinal axis of inertia
and the wind axis.

In order to obtain an experimental check of lateral-stability
calculations including the product-of-inertia terms, a systematic
series of flight tests have been made in the Langley free-flight
tunnel. A model having a 42° sweptback wing was used to determine
experimentally the effects of the product of inertia on the lateral
stability of the free-flying model for correlation with the cal-
culated stability characteristics of the model. In order to
provide a comprehensive check of the calculations, the directional
stability of the model was varied by changing the vertical-tail
size and tail length and the quantitative effects of the product
of inertia were varied by changing the wing incidence and thereby
changing the inclination of the principal axes of inertia relative to
the wind axes.

SYMBOLS

The forces and moments are referred to the stability axes, which
are defined as an orthogonal system of axes intersecting at the
airplane center of gravity in which the Z-axis is in the plane of
symmetry and perpendicular to the relative wind, the X-axis is in
the plane of symmetry and perpendicular to the Z-axis, and the
Y-axis is perpendicular to the plane of symmetry. A diagram of
these axes showing the positive direction of forces and moments
is presented in figure 1.

The symbols and coefficients are defined as follows:

W   weight of model, pounds

m   mass of model, slugs

S   wing area, square feet

S_t vertical-tail area, square feet

b   wing span, feet

c   wing chord, feet

l tail length (distance from center of gravity to
               rudder hinge line), feet

$\bar{z}$ height of center of pressure of vertical tail above fuselage axis, feet

i_w angle of incidence of wing, degrees

k_X radius of gyration of model about principal longitudinal axis, feet

k_Z radius of gyration of model about principal normal axis, feet

k_{XZ} product-of-inertia factor, feet^2 $\left(\left(k_Z^2 - k_X^2\right) \cos \eta \sin \eta\right)$

η angle of attack of principal longitudinal axis of airplane; positive when forward end of major principal axis is above X-axis

V airspeed, feet per second

q dynamic pressure, pounds per square foot $\left(\frac{1}{2}\rho V^2\right)$

p rolling angular velocity, radians per second

r yawing angular velocity, radians per second

ρ mass density of air, slugs per cubic foot

β angle of sideslip, degrees except where otherwise noted

α angle of attack of fuselage axis, degrees

γ angle of climb, degrees

μ airplane relative-density factor $\left(\frac{m}{\rho Sb}\right)$

C_L lift coefficient $\left(\frac{\text{Lift}}{qS}\right)$

C_Y lateral-force coefficient $\left(\frac{\text{Lateral force}}{qS}\right)$

C_l rolling-moment coefficient $\left(\frac{\text{Rolling moment}}{qSb}\right)$

C_n yawing-moment coefficient $\left(\frac{\text{Yawing moment}}{qSb}\right)$

C_{Y_β} rate of change of lateral-force coefficient with angle of sideslip in radians $\left(\frac{\partial C_Y}{\partial \beta}\right)$

C_{l_β} rate of change of rolling-moment coefficient with angle of sideslip in radians (except where specified to be in degrees) $\left(\dfrac{\partial C_l}{\partial \beta}\right)$

C_{n_β} rate of change of yawing-moment coefficient with angle of sideslip in radians (except where specified to be in degrees) $\left(\dfrac{\partial C_n}{\partial \beta}\right)$

C_{Y_p} rate of change of lateral-force coefficient with rolling-angular-velocity factor in radians $\left(\dfrac{\partial C_Y}{\partial \dfrac{pb}{2V}}\right)$

C_{l_p} rate of change of rolling-moment coefficient with rolling-angular-velocity factor in radians $\left(\dfrac{\partial C_l}{\partial \dfrac{pb}{2V}}\right)$

C_{n_p} rate of change of yawing-moment coefficient with rolling-angular-velocity factor in radians $\left(\dfrac{\partial C_n}{\partial \dfrac{pb}{2V}}\right)$

C_{l_r} rate of change of rolling-moment coefficient with yawing-angular-velocity factor in radians $\left(\dfrac{\partial C_l}{\partial \dfrac{rb}{2V}}\right)$

C_{n_r} rate of change of yawing-moment coefficient with yawing-angular-velocity factor in radians $\left(\dfrac{\partial C_n}{\partial \dfrac{rb}{2V}}\right)$

APPARATUS

The investigation was conducted in the Langley free-flight tunnel, which is equipped for testing free-flying dynamic airplane models. A description of the tunnel and its operation is given in references 3 and 4. Free-oscillation tests were made to determine the damping-in-yaw derivative C_{n_r} by the method described in reference 5. Steady-rotation tests were made to determine the damping-in-roll deriva-tive C_{l_p} by the method described in reference 6.

A sketch of the model used in the investigation is shown as figure 2. This model is described in reference 7 except for a few changes which were necessary for the present investigation. Wedge-shape blocks were provided in order that the wing might be mounted

on the fuselage with $0°$, $10°$, and $-10°$ incidence. The model was equipped with a set of interchangeable vertical tails, ranging in size from 2.6 to 10.4 percent of the wing area, which could be mounted at any of the three tail-length positions indicated in figure 2. The various model configurations tested are identified in table I.

TESTS AND CALCULATIONS

Force tests of the model were made to determine the values of static-lateral-stability derivatives with various vertical-tail arrangements and wing incidences. Flight tests of the model were made at a lift coefficient of 0.6 with angles of incidence of the wing of $0°$, $10°$, and $-10°$ and with vertical-tail arrangements given in table I that provide the values of the directional-stability parameter C_{n_β} and the effective dihedral parameter $-C_{l_\beta}$ indicated in figure 3.

The model was flown at each test condition to determine the stability of the Dutch roll oscillation, which was recorded by photographing the uncontrolled motions of the model after a disturbance caused by abruptly deflecting the ailerons to roll the model from approximately $30°$ bank to level flight and then centering the controls. In some of the cases the flying characteristics of the model were too poor to permit recording the uncontrolled motions of the model and it was necessary to resort to the pilot's observations to determine whether the model was stable. The pilot's impression of the general flying characteristics of the model were also noted in order to provide data concerning the ease of flying the model, both for level flight and for performance of the mild maneuvers possible in the tunnel. The ratings of the general flying characteristics of the model in controlled flight generally indicate whether stability and controllability are adequate and properly proportioned. The vertical-tail area and tail length were selected in an attempt to bracket the oscillatory-stability boundaries in order to provide the desired correlation of test and theory.

All the flight tests were made with the rudder coupled to the ailerons for lateral control, and the ratio of rudder deflection to aileron deflection was adjusted for each test condition to minimize the adverse yawing due to rolling and aileron deflection. For the lower values of directional stability, however, the adverse yawing could not be entirely eliminated.

Calculations were made by the method presented in reference 2 to determine the boundary of neutral stability of the lateral oscillation of the model. Two sets of calculations were made, one taking into consideration and the other neglecting the product of inertia. The boundaries for the model with a 10° angle of incidence of the wing were computed by assuming changes of the tail size, and the boundaries for the model with 0° and -10° angles of incidence of the wing were computed by assuming changes in the tail length in order to make the calculations consistent with the test procedure.

The aerodynamic and mass characteristics of the model used in the calculations are presented in table II. The mass characteristics of the model were obtained by measurements. The inclination of the principal longitudinal axis of inertia to the fuselage axis was found to be less than 0.3° for all wing incidences and was assumed to be zero in the calculations. The trim airspeed, flight-path angle, and angle of attack were determined from free-flight tests. The values of C_{Y_β} (tail off) and C_{n_β} (tail off) were obtained from force tests. The values of $C_{Y_{\beta(tail)}}$ for configurations B and C were also obtained from force tests. (See table II.) The tail-off values of C_{l_p} and C_{n_r} were determined from steady-rotation and free-oscillation tests, respectively; and the tail-off values of C_{l_r} and C_{n_p} were estimated from the charts of reference 8 and unpublished wind-tunnel data. The tail contributions to the stability derivatives were estimated from the equations given in the footnote of table II, which are similar to those given in reference 9, by utilizing the experimentally determined values of C_{Y_β} contributed by the vertical tails and the arbitrarily chosen values of tail length in the case of configurations B and C and by utilizing the given tail length and arbitrarily chosen values of $C_{Y_{\beta(tail)}}$ in the case of configuration A.

RESULTS AND DISCUSSION

Stability

The results of the stability investigation are presented in figures 3 and 4. Figure 3 shows the calculated oscillatory-stability boundaries of the model and indicates whether the uncontrolled lateral oscillations of the model were stable, neutral, or unstable in the configurations tested. Figure 4 shows typical time histories of the uncontrolled rolling motion of the model following a rolling

disturbance. Only the rolling motions are presented for simplicity. The period and damping of the rolling motions, however, are identical with those of the yawing and sideslipping. Inasmuch as spiral stability is considered relatively unimportant and the calculations indicate no effect of the products of inertia, the spiral stability of the model was not investigated.

When the product of inertia terms were included in the calculations of the stability boundaries, the boundaries were in good agreement with the flight test results as shown in figures 3(a) and 3(b). Figure 3(c) shows that the model was stable, as is indicated by the calculated stability boundary which included product of inertia. However, it was impossible to check this boundary closely because the model could not be flown at negative values of C_{n_β}. A simple illustration of the pronounced effect of the product of inertia may be obtained by a comparison of test points for configurations A_3 and B_1 in which the model configurations were identical except for the change in wing incidence and the consequent change in the angle of attack of the principal longitudinal axis of inertia. In configuration A_3 ($i_w = 10^\circ$) the model was unstable whereas in configuration B_1 ($i_w = 0^\circ$) the model was quite stable.

The test results are at variance with the stability boundaries which were calculated by neglecting the product of inertia. This difference is particularly evident in figures 3(b) and 3(c). Some additional calculations were made in order to insure that poor estimates of the stability derivatives which were not measured could not account for the discrepancy between the test results and the calculations in which the product of inertia was neglected. The results of the calculations are presented in figure 5 which shows the effects on the stability boundary of introducing a large value of the stability derivative C_{Y_p}, doubling the tail-off value of C_{l_r}, or using one-half the estimated value of C_{n_p} (tail off). None of these changes in the stability derivatives could account for more than approximately one-fourth of the difference between the calculations neglecting the product of inertia terms and the point of neutral stability as determined from the tests. The product of inertia terms should therefore be included in lateral-stability calculations.

The stability or instability of the uncontrolled motions of the models, as shown in figure 4, was quite definite except for test configuration B_3 which appears to be about neutrally stable. No

records of the uncontrolled lateral motions could be made for the
condition of -10° wing incidence because the poor flying charac-
teristics of the model with so little directional stability made
such records very difficult to obtain. The pilot's impression
was, however, that the lateral oscillations of the model for these
conditions were heavily damped.

The data of figures 3 and 4 are in good agreement with refer-
ence 2 regarding the pronounced effects of the product of inertia
on lateral stability. At the present time there are not sufficient
data to determine when the effects of the product of inertia will
be important; hence, the product of inertia should be considered
in all lateral-stability analyses.

General Flight Behavior

The flight-test results presented in figure 6 show that the
general flight behavior of the model was influenced primarily by
the static directional stability, which has a pronounced effect
on the response of the model to the controls, and to a lesser degree
by the dynamic lateral stability.

At constant C_{n_β}, increasing the oscillatory stability by
decreasing the wing incidence improved the general flight behavior
of the model because an increase in the stability increases the
tendency of the model to fly itself and thereby makes the piloting
of the model easier and the flight smoother. The most apparent
effect of the oscillatory stability on the general flight behavior
was found by comparing the flying characteristics of configurations A_3
and B_1.

Increasing the directional stability improved the general
behavior of the model by improving the response to controls as
was explained in reference 10. This effect was especially noticeable
with the present model because of the high effective dihedral of the
model. When adverse yawing occurred this high effective dihedral
produced rolling moments which opposed the aileron rolling moments
and thus reduced the effectiveness of the ailerons for controlling
the model. The data presented in figure 6 show that the model was
easier to fly in configurations A_2 and A_3 than in configurations B_2
and B_3, in spite of the fact that the lateral oscillations were
unstable for the A configurations and stable or neutrally stable
for the B configurations. The directional stability of the model
was too low for satisfactory response to the controls in configura-
tions B_2 and B_3. For configuration C_3 the response of the model
to the controls was so poor that it was virtually unflyable although

the lateral oscillations were apparently very stable, as was indicated by the calculations. The model could not be flown with any less directional stability than it had in configuration C_3.

It was therefore concluded that general flight behavior was influenced primarily by static directional stability and to a lesser degree by the dynamic lateral stability and that a certain minimum amount of static directional stability was required to give good response to the controls even when less directional stability provided good damping of the lateral oscillations.

CONCLUSIONS

The following conclusions were drawn from an investigation in the Langley free-flight tunnel to obtain a correlation between the calculated and the measured effects of the product of inertia on lateral stability characteristics:

1. The calculated lateral-stability boundaries were in good agreement with measured lateral stability when the product of inertia terms were included in the calculations. Neglecting the product of inertia, however, led to wide discrepancies between calculated and measured stability. These results emphasized the necessity for considering the product of inertia in lateral-stability analyses.

2. The general flying characteristics were influenced primarily by the static directional stability and to a lesser degree by the stability of the lateral oscillations. A certain minimum amount of static directional stability was required to give good controllability even when less directional stability provided good damping of the lateral oscillations.

Langley Memorial Aeronautical Laboratory
    National Advisory Committee for Aeronautics
        Langley Field, Va., May 21, 1947

REFERENCES

1. Zimmerman, Charles H.: An Analysis of Lateral Stability in Power-Off Flight with Charts for Use in Design. NACA Rep. No. 589, 1937.

2. Sternfield, Leonard: Effect of Product of Inertia on Lateral Stability. NACA TN No. 1193, 1947.

3. Shortal, Joseph A., and Osterhout, Clayton J.: Preliminary Stability and Control Tests in the NACA Free-Flight Wind Tunnel and Correlation with Full-Scale Flight Tests. NACA TN No. 810, 1941.

4. Shortal, Joseph A., and Draper, John W.: Free-Flight-Tunnel Investigation of the Effect of the Fuselage Length and the Aspect Ratio and Size of the Vertical Tail on Lateral Stability and Control. NACA ARR No. 3D17, 1943.

5. Campbell, John P., and Mathews, Ward O.: Experimental Determination of the Yawing Moment Due to Yawing Contributed by the Wing, Fuselage, and Vertical Tail of a Midwing Airplane Model. NACA ARR No. 3F28, 1943.

6. Bennett, Charles V., and Johnson, Joseph L.: Experimental Determination of the Damping in Roll and Aileron Rolling Effectiveness of Three Wings Having 2°, 42°, and 62° Sweepback. NACA TN No. 1278, 1947.

7. Maggin, Bernard, and Bennett, Charles V.: Flight Tests of an Airplane Model with a 42° Swept-Back Wing in the Langley Free-Flight Tunnel. NACA TN No. 1287, 1947.

8. Pearson, Henry A., and Jones, Robert T.: Theoretical Stability and Control Characteristics of Wings with Various Amounts of Taper and Twist. NACA Rep. No. 635, 1938.

9. Bamber, Millard J.: Effect of Some Present-Day Airplane Design Trends on Requirements for Lateral Stability. NACA TN No. 814, 1941.

10. McKinney, Marion O., Jr.: Experimental Determination of the Effects of Dihedral, Vertical-Tail Area, and Lift Coefficient on Lateral Stability and Control Characteristics. NACA TN No. 1094, 1946.

TABLE I

VERTICAL-TAIL ARRANGEMENTS FOR THE VARIOUS

MODEL CONFIGURATIONS

Model configuration	Wing incidence, i_w (deg)	Vertical-tail area, S_t/S	Tail length, l/b
A_1	10	0.104	0.67
A_2	10	.078	.67
A_3	10	.052	.67
B_1	0	.052	.67
B_2	0	.052	.41
B_3	0	.052	.15
C_1	-10	.026	.67
C_2	-10	.026	.41
C_3	-10	.026	.15

NATIONAL ADVISORY
COMMITTEE FOR AERONAUTICS

TABLE II

CHARACTERISTICS OF THE MODEL USED IN THE CALCULATIONS

	Configuration A	Configuration B	Configuration C
i_W	10.0	0	-10.0
W	5.10	4.64	5.10
W/S	2.04	1.855	2.04
b	3.82	3.82	3.82
ρ	0.00238	0.00238	0.00238
V	53.5	51.2	53.5
μ	7.00	⌣.34	7.00
k_X	0.475	0.510	0.475
k_Z	1.315	1.290	1.315
k_{XZ}	0.0447	-0.191	-0.438
l/b	0.67	[b]Variable	[b]Variable
$\bar{z}/b$	$0.1345\sqrt{C_{Y_{\beta(tail)}}}$	0.072	0.036
C_L	0.6	0.6	0.6
α	-4.0	6.0	16.0
γ	-9.0	-9.0	-9.0
C_{Y_β}	$-0.0074 + C_{Y_{\beta(tail)}}$	$-0.0074 + C_{Y_{\beta(tail)}}$	$-0.0074 + C_{Y_{\beta(tail)}}$
[a]C_{n_β}	$0 + C_{n_{\beta(tail)}}$	$0 + C_{n_{\beta(tail)}}$	$0 + C_{n_{\beta(tail)}}$
[a]C_{l_p}	$-0.230 + C_{l_{p(tail)}}$	$-0.230 + C_{l_{p(tail)}}$	$-0.230 + C_{l_{p(tail)}}$
[a]C_{n_p}	$-0.0332 + C_{n_{p(tail)}}$	$-0.0332 + C_{n_{p(tail)}}$	$-0.0332 + C_{n_{p(tail)}}$
[a]C_{l_r}	$0.125 + C_{l_{r(tail)}}$	$0.125 + C_{l_{r(tail)}}$	$0.125 + C_{l_{r(tail)}}$
[a]C_{n_r}	$-0.0090 + C_{n_{r(tail)}}$	$-0.0090 + C_{n_{r(tail)}}$	$-0.0090 + C_{n_{r(tail)}}$
$C_{Y_{\beta(tail)}}$	[b]Variable	-0.1870	-0.0784

[a]Tail contributions are determined from the following equations:

$$C_{n_{\beta(tail)}} = -\frac{l}{b}\,C_{Y_{\beta(tail)}}$$

NATIONAL ADVISORY
COMMITTEE FOR AERONAUTICS

$$C_{l_{p(tail)}} = 2\left(\frac{\bar{z}}{b} - \frac{l}{b}\sin\alpha\right)^2 C_{Y_{\beta(tail)}}$$

$$C_{n_{p(tail)}} = C_{l_{r(tail)}} = -2\,\frac{l}{b}\left(\frac{\bar{z}}{b} - \frac{l}{b}\sin\alpha\right)C_{Y_{\beta(tail)}}$$

$$C_{n_{r(tail)}} = 2\left(\frac{l}{b}\right)^2 C_{Y_{\beta(tail)}}$$

[b]Varied systematically as independent variable to provide the desired range of C_{n_β} for the determination of the stability boundaries.
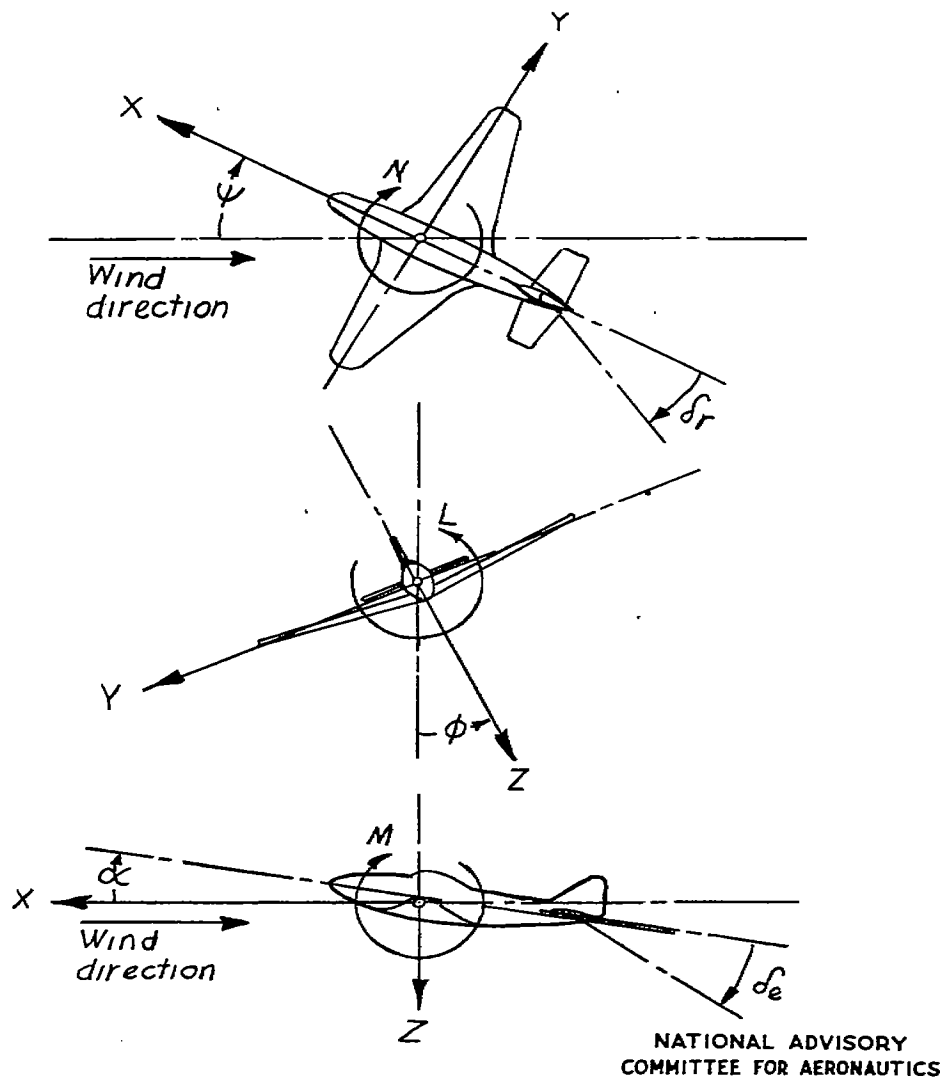
Figure 1. - The stability system of axes. Arrows indicate positive directions of moments, forces, and control-surface deflections. This system of axes is defined as an orthogonal system having their origin at the center of gravity and in which the Z-axis is in the plane of symmetry and perpendicular to the relative wind, the X-axis is in the plane of symmetry and perpendicular to the Z-axis, and the Y-axis is perpendicular to the plane of symmetry.
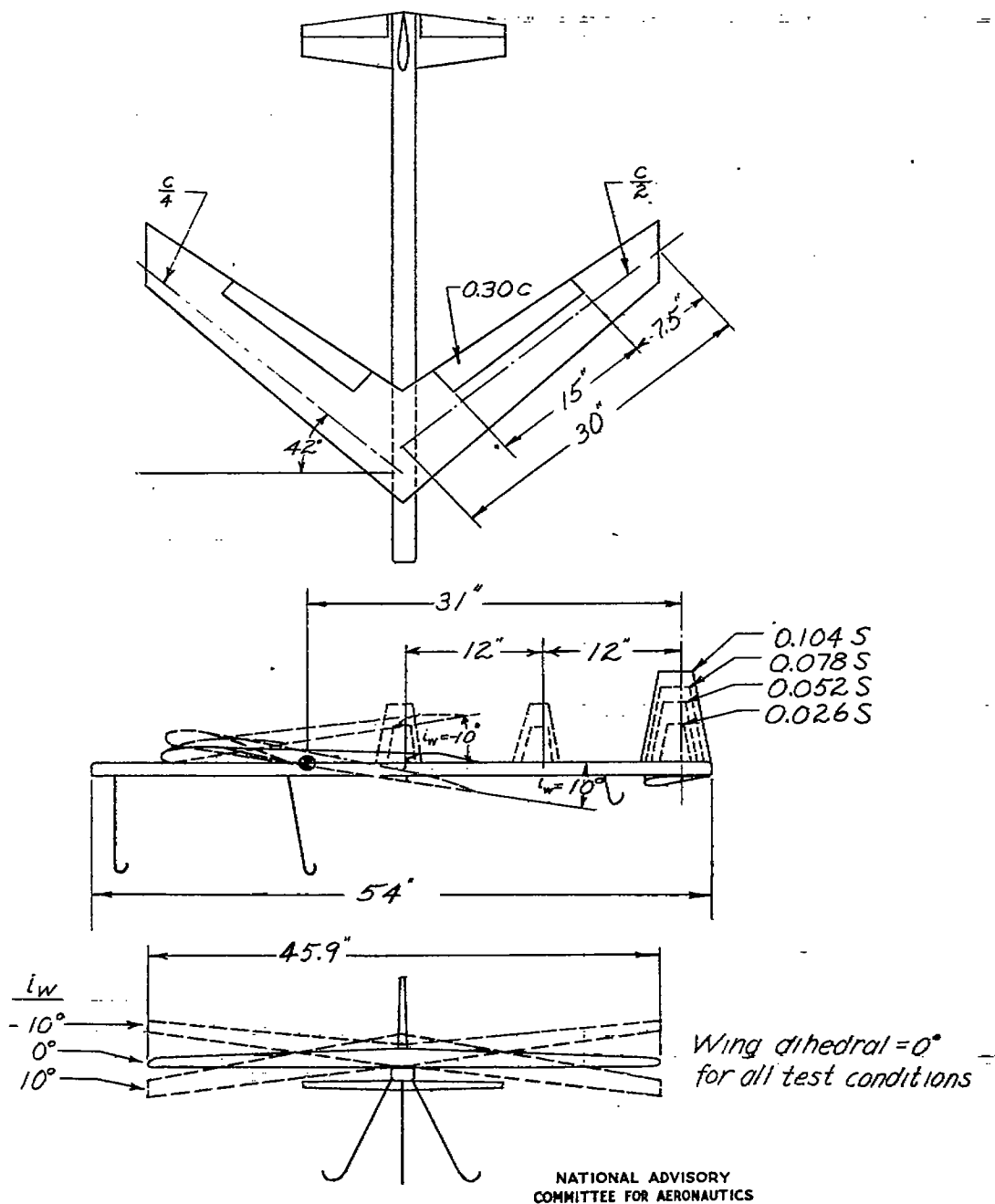
Fig. 2   NACA TN No. 1370

Figure 2.—Three-view sketch of model used
in product-of-inertia investigation.
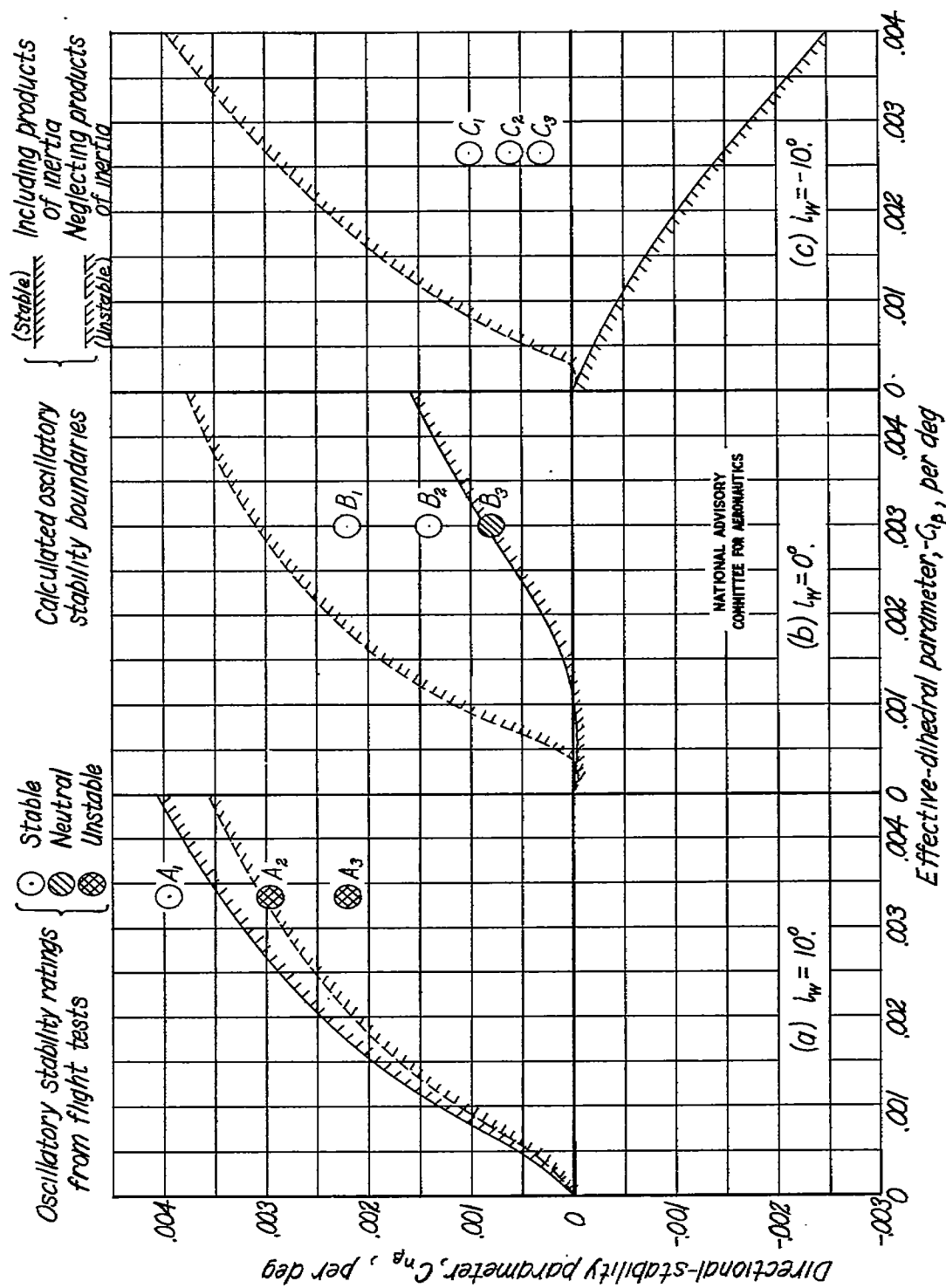
Figure 3.— Correlation of oscillatory-stability ratings from flight tests with calculated oscillatory-stability boundaries.
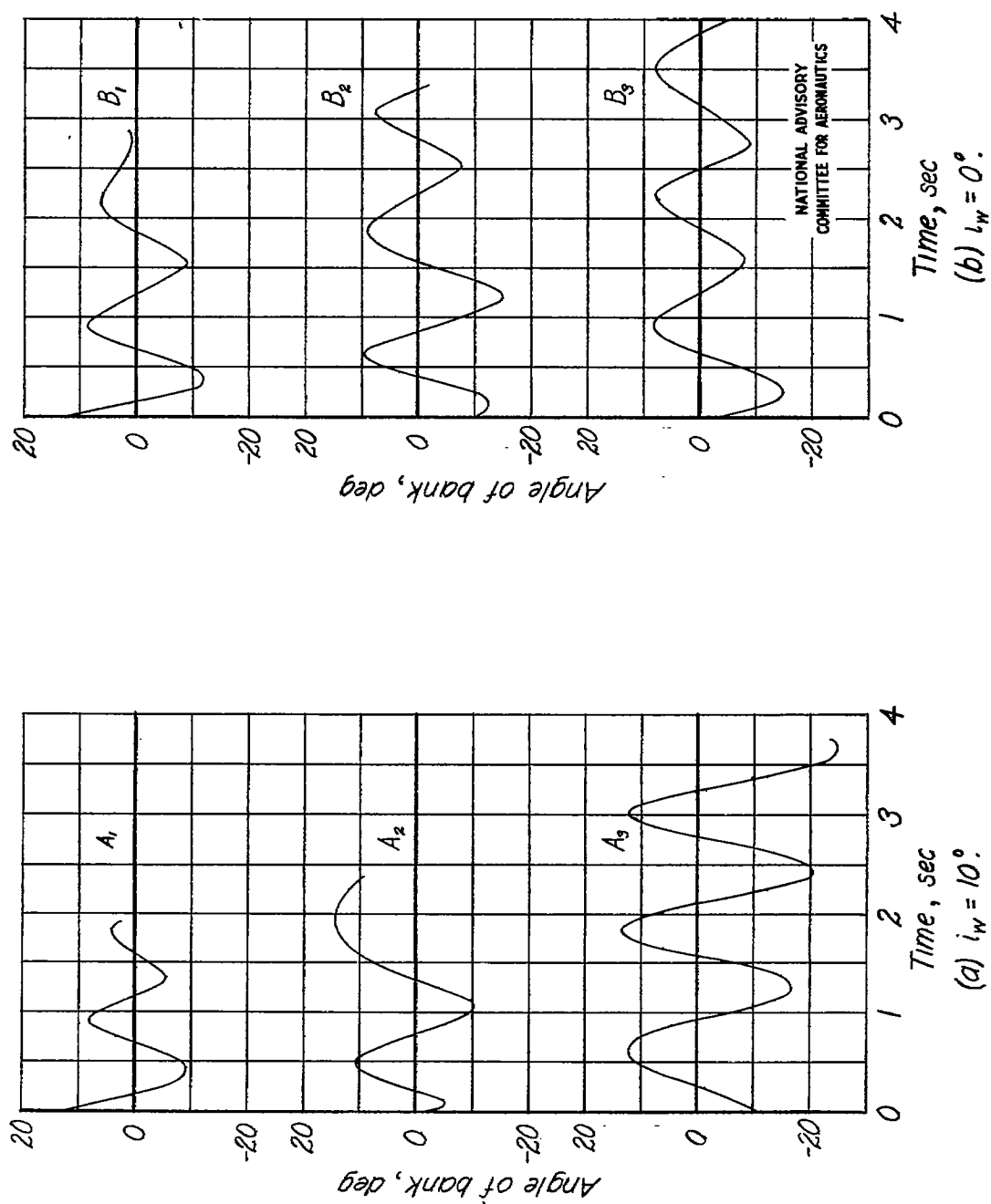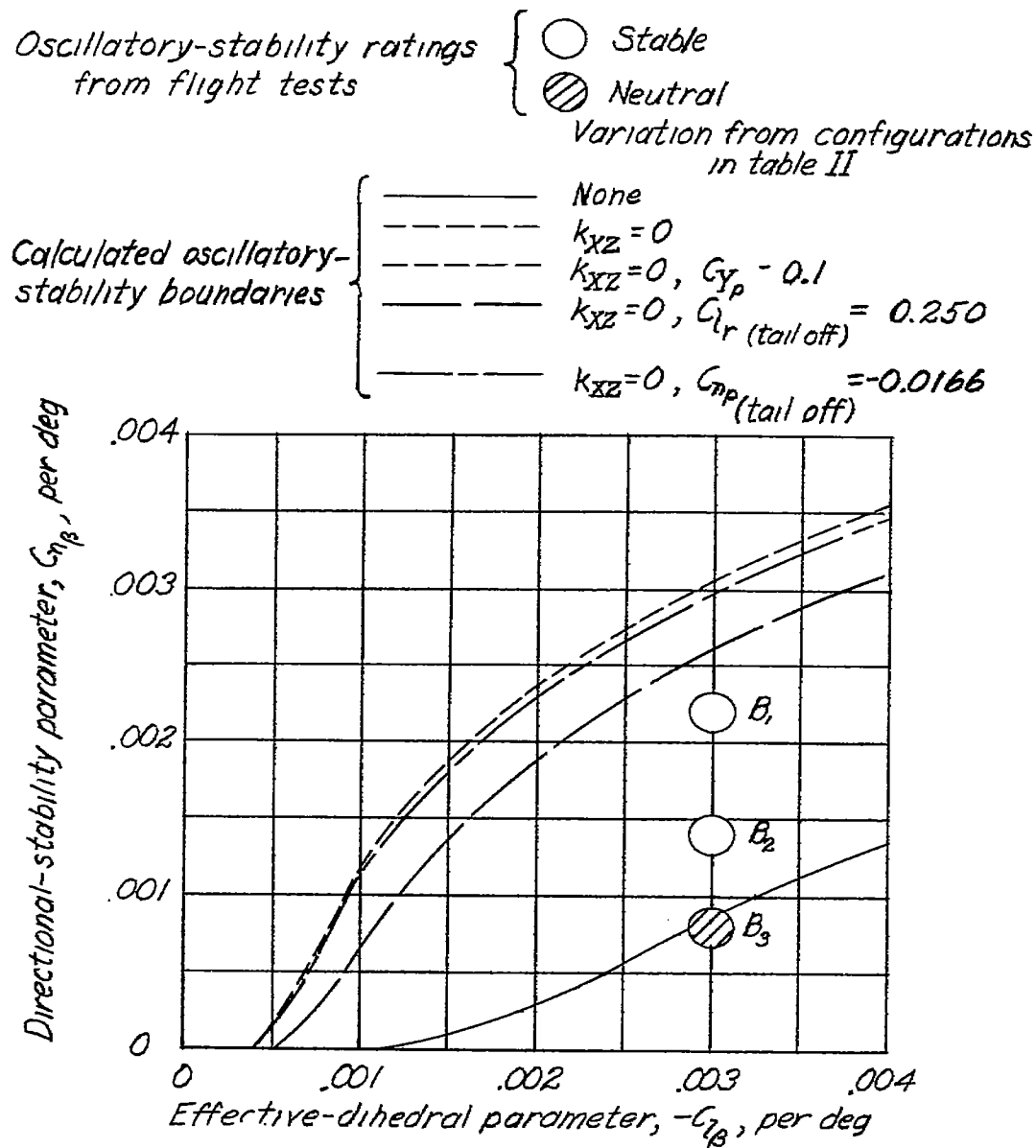
Fig. 4　　　　　　　　　　　　　　　　　　　NACA TN No. 1370

Figure 4.— Flight records of the uncontrolled rolling motions of the model.

Figure 5.— Effect of varying some of the stability derivatives on the oscillatory-stability boundaries $(i_w = 0°)$.
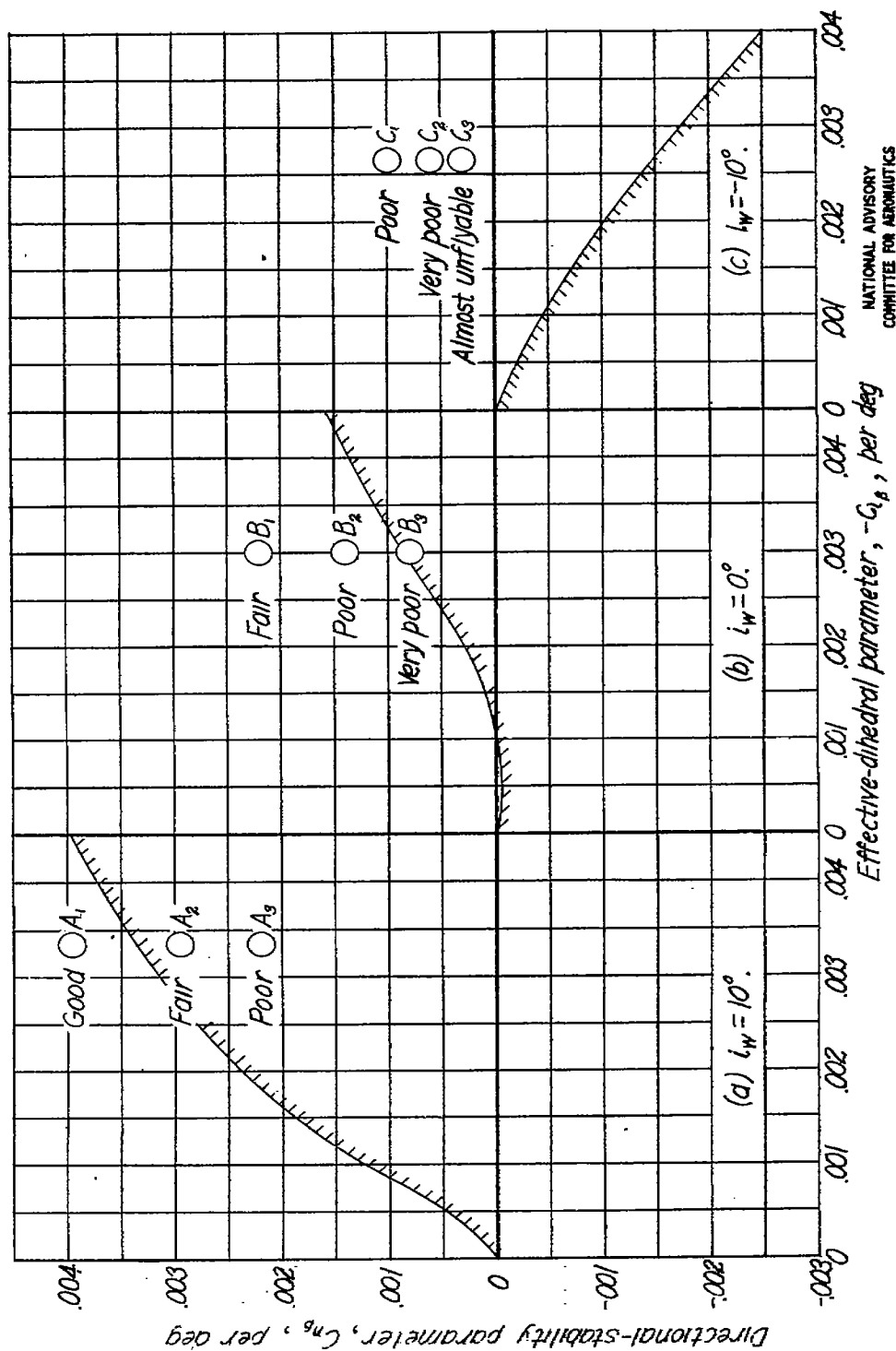
Fig. 6   NACA TN No. 1370

Figure 6.— General flight-behavior ratings from flight tests of the model.